# Assembly and Post-Modification of a Metal–Organic Nanotube for Highly Efficient Catalysis

Guo-Qiang Kong, Sha Ou, Chao Zou, and Chuan-De Wu*

Department of Chemistry, Zhejiang University, Hangzhou 310027, P.R. China

Ⓢ *Supporting Information*

ABSTRACT: A metal–organic nanotube (MONT) was synthesized by linking up the bent organic ligands and the tetra-coordinated zinc cations under mild conditions. Structural analysis revealed that the MONT has a very large exterior wall diameter of 4.91 nm and an interior channel diameter of 3.32 nm. Interlocking of the nanotubes gives rise to a 3D chiral framework containing 1D helical cylindered channels with diameter of 2.0 nm. The MONT has very interesting property by synergizing the functionality of nanotubes, metal–organic frameworks (MOFs), and N-heterocyclic carbenes (NHCs). The dye adsorption experiments demonstrate that the channels of the MONTs are accessible to large reagents typically used for catalysis. The postmodification of the MONT can be easily operated by unmarking the imidazolium moieties in the channel walls, which was conducted as a highly active heterogeneous catalyst for Suzuki–Miyaura and Heck coupling reactions, hydrogenation of olefins and nitrobenzene, while the constituent elements are less efficient for these reactions under the same conditions.
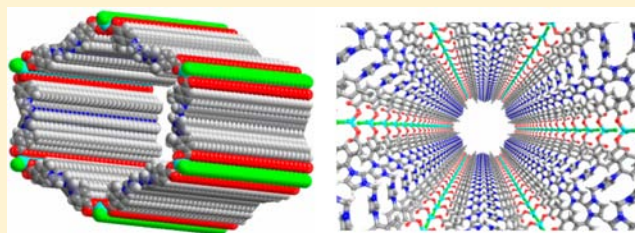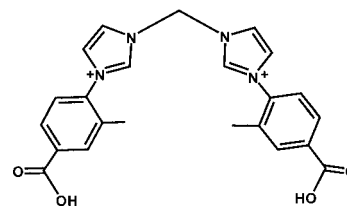
■ INTRODUCTION

Synthesis of discrete nanotubular materials has attracted great interest following the discovery of carbon nanotubes (CNTs).[1] Many inorganic, organic, and biologic materials have been used as functional precursors for the construction of synthetic nanotubes (SNTs). CNTs and SNTs represent a remarkable class of functional materials for a number of applications as molecular capillaries, sieves, catalysts, electrodes, and biological models.[2,3] However, precise control of the functionality of SNTs remains a challenging task due to their extreme synthesis conditions. Compared with those of CNTs and SNTs, the functionality of metal–organic frameworks (MOFs) is easily controlled by tailoring their building constituents and functional groups. The MOF materials have been realized applications in diverse fields of gas storage, separation, catalysis, sensing, and drug delivery.[4] Moreover, the variety and complexity of organic building blocks make it possible to design and synthesize metal–organic nanotubes (MONTs) as analogues of SNTs.[5−7] There are quite a few three-dimensional (3D) MOFs that contain 1D nanotubular channels; however, only few examples are discrete MONTs, especially post-modifiable MONTs.[6,7]

Because N-heterocyclic carbenes (NHCs) are excellent *s*-donors and weak *p*-acceptors, they are used to combine with diverse metal atoms for a number of applications. It is interesting to note that the NHC-based catalysts are highly active and very stable under various conditions and are much superior to the phosphine-based catalysts.[8,9] Recent elaboration demonstrates that the MOF materials based on NHCs or their precursors of azoliums have interesting properties that associate with the distinctive functions of MOFs and NHCs.[10,11]

We are greatly interested in the synthesis of discrete MONTs with functional NHCs for catalytic application, because such MONT materials might synergize the characters of MOFs, SNTs, and NHCs to give rise to unusual properties. Considering that the structures of MONTs are largely dependent on the configurations and coordination donors of organic linkers, we therefore designed a bent 1,1′-methylenebis-(3-(4-carboxy-2-methylphenyl)-1*H*-imidazol-3-ium) (H₂L) ligand containing two charged aromatic azoliums (Scheme 1).

Scheme 1. Schematic Representation of the H₂L Ligand

The two methyl groups and the bent geometry of the ligand can direct the metal–ligand orientation for the formation of discrete MONTs. Moreover, introduction of the two imidazolium moieties in the ligand let the tailorability of MONTs be more practical than that of traditional MOFs, because it is difficult to find the postmodification conditions for traditional MOFs that give the requisite properties. Herein we report a novel chiral MONT of $[ZnLCl_2]\cdot 8H_2O$ (**1**) with a very large exterior wall diameter of 4.91 nm and an interior channel

diameter of 3.32 nm. MONT **1** can be easily deprotonized to anchor palladium atoms by unmasking the imidazolium moieties under mild conditions. The selective dye adsorption experiments demonstrate that the channels are accessible to large substrates typically used in the catalysis. The catalytic experiments showed that the postmodified solid is highly efficient for Suzuki–Miyaura and Heck cross-coupling reactions and for hydrogenation of olefins and nitrobenzene under mild conditions.

■ RESULTS AND DISCUSSION

Colorless crystals of compound **1** were synthesized by the reaction of H_2LCl_2 and $Zn(NO_3)_2 \cdot 6H_2O$ in a mixed solvent of H_2O and EtOH at room temperature for three days. The crystalline solid of **1** can be obtained in a range of pH values (4−8) and ligand-to-metal ratios. The different reaction conditions are responsible for the sizes of the needle-shaped crystals. The phase purity of the bulky samples was confirmed by powder X-ray diffraction (PXRD) study. We also tried to synthesize crystals in other solvent media, such as water, DMF, etc. However, no crystalline sample was produced. The crystals of **1** are slightly soluble in water but very stable in common organic solvents, such as EtOH, MeOH, THF, and DMF, etc. The formula of compound **1** was figured out on the basis of single-crystal diffraction and elemental and thermogravimetric analysis (TGA).

Single-crystal X-ray diffraction analysis revealed that compound **1** crystallizes in the hexagonal chiral $P6_222$ space group. Each Zn^{II} atom coordinates to two carboxyl oxygen atoms ($Zn-O = 1.977(6)$ Å) of two **L** ligands and two chlorine atoms ($Zn-Cl = 2.278(2)$ Å) in a distorted tetrahedral coordination geometry. The bidentate **L** ligands link up Zn^{II} metal nodes to form a right-handed helical chain, which is intertwined itself with a period of 15.42 Å running along the screw 6_2 axis (Figure 1a).

The most intriguing feature of **1** is the single-walled MONT formed from double-helices (Figure 1b−d). A top view of the open-ended hollow chiral nanotube indicates that it is a pseudohexanuclear $\{Zn_6L_6Cl_{12}\}$ metallomacrocycle. Each $Zn\cdots Zn$ separation, bridged by the **L** ligand, is 22.70(1) Å. It is noteworthy that the MONT has a large cross section with an exterior wall diameter of 4.91 nm and an interior channel diameter of 3.32 nm (considering the van der Waals radii).

The chiral MONT further intertwines with six helical nanotubes to give rise to a periodically ordered interlocked framework, which is stabilized by the van der Waals contacts (Figure 1e and f). Interlocking of the nanotubes leads to a 3D chiral framework with the eclipsing of nanotube margins. The diameter of the 1D chiral cylindered channels is 2.0 nm (considering the van der Waals radii). PLATON calculations suggest that **1** contains 47.2% void space that is accessible to the solvent molecules.[12] TGA of **1** indicates that a weight loss of 19.8% occurred between 30 and 175 °C, corresponding to the loss of lattice water molecules (expected 20.7%).

It is interesting to note that the imidazolium moieties in the 1D channels of **1** are readily available to be deprotonated for the formation of NHCs by postmodification. The process was conveniently performed by treating **1** with $Pd(OAc)_2$ in THF solvent. The newly formed light-brown solid **2** is more stable than compound **1**. It is insoluble in common organic solvents and water. To check whether a Pd−carbene derivative formed, a sample of solid **2** was digested by using a diluted aqueous HCl solution. ^1H NMR study showed that the ratio of **L** to **L′** (**L′**
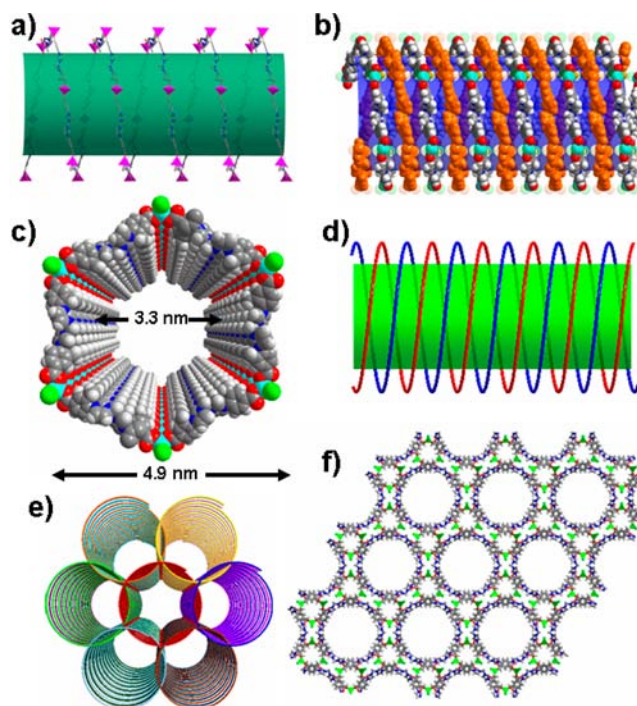

Figure 1. (a) Side-view of the right-handed helical chain. (b) Space-filling representation of the single-walled MONT based on double-helices. (c) Perspective view of the open-ended hollow chiral nanotube. (d) Schematic representation of the double-helices. (e) Schematic representation of intertwined nanotubes. (f) Packing diagram of **1**, showing the 1D opening channels as viewed along the *c* axis.

refers to deprotonated **L**) is about 42:58 (see Supporting Information [SI], Figure S44). Inductively coupled plasma mass spectrometry (ICP-MS) revealed that solid **2** contains 7.8% palladium, which is consistent with the ^1H NMR integration. The photoluminescent spectrum of **1** exhibits a broad emission band around 317 nm upon excitation at 270 nm, which is similar to that of H_2LCl_2. However, the emissions are significantly weakened in the photoluminescent spectra of **2** and $H_2L′/Pd$. These results further proved the combination of Pd atoms and NHCs of **L′** in **2**. To check whether Pd^{II} cations were partially reduced for the formation of Pd^0 nanoparticles in **2**, we therefore conducted TEM experiments. A comparison of the TEM images of **1** and **2** suggests that there is no distinctly congregated Pd^0 nanoparticle in **2**. The X-ray photoelectron spectrum (XPS) of **2** showed that the binding energies for Pd $3d_{5/2}$ and $3d_{3/2}$ are 337 and 342 eV, respectively. The binding energies are characteristic for divalent Pd and not for a peak corresponding to zerovalent species that should locate around 335 and 340 eV in the $3d_{5/2}$ and $3d_{3/2}$ levels, respectively.[13−15] Encapsulating free $Pd(OAc)_2$ in the solid can also be eliminated because the Pd $3d_{5/2}$ binding energy in $Pd(OAc)_2$ is 338.7 eV.[15] The identical PXRD patterns of **1** and **2** suggest that the framework structure remains after the postmodification. In a word, all of the above results unambiguously proved that the imidazolium moieties in **1** are partially deprotonated for the formation of Pd^{II}−NHCs in **2** with retained framework structure.

Whereas the catalytic application of porous materials requires that the channels and catalytic sites are accessible by substrate molecules to facilitate heterogeneous catalysis, a dye-uptake assay was thus employed to quantify the intrinsic porosity of
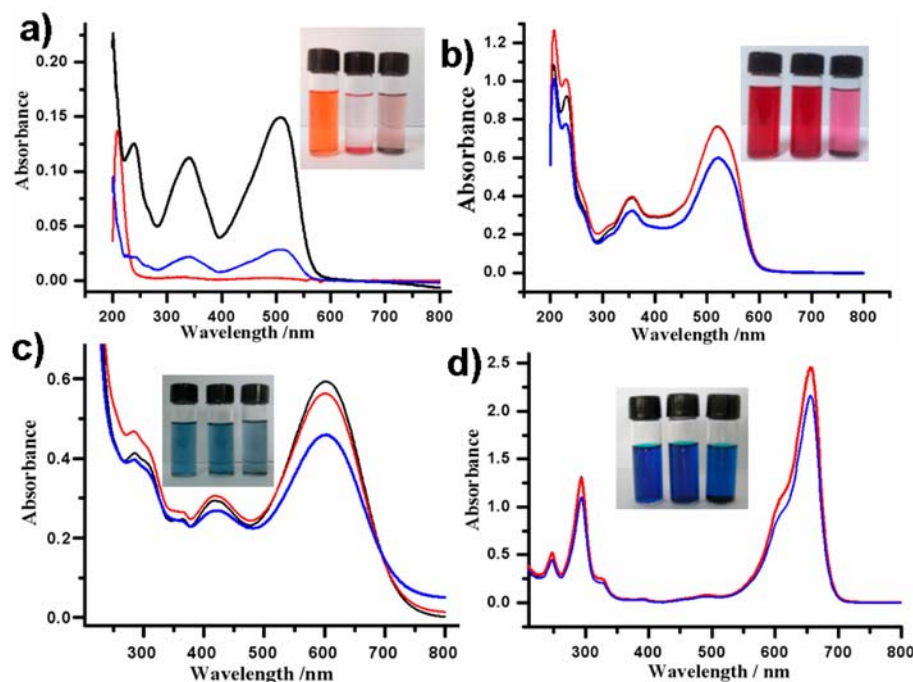
Figure 2. UV−vis spectra of (a) Congo Red, (b) Oil Red O, (c) Sudan Black B, and (d) Methylene Blue before (black lines) and after (red line for **1** and blue line for **2**) the addition of solids **1** and **2**. (Insets) Photographs highlight the sorption effects. Left: before sorption, Middle: after sorption by **1**, Right: after sorption by **2**).

the two MONTs by taking advantage of the nanoscaled open channels and the zwitterionic nature.[16] When the samples of **1** and **2** were respectively added into ethanol solutions of Congo Red, Oil Red O, Sudan Black B, and Methylene Blue for 24 h at room temperature, the solids presented distinct adsorption ability for these dyes as monitored by UV−vis absorption spectroscopy (Figure 2). The dye uptakes of **1** and **2** were respectively 10.0 and 8.3 wt % for Congo Red, 0.09 and 1.4 wt % for Oil Red O, 0.55 and 0.95 wt % for Sudan Black B, and 0.24 and 1.46 wt % for Methylene Blue. Because the channel dimensions of the MONTs are large enough to swallow these dyes (see SI, Figures S39−S42), the host−guest (sorbate−sorbent) interaction should be a dominant effect for the distinct dye uptakes.[17] The positively charged imidazolium moieties in the channels have high affinity for the anionic Congo Red molecules, while the neutral and cationic dyes of Oil Red O, Sudan Black B, and Methylene Blue are not the favored guests. Since the maximum UV−vis absorption peaks of Congo Red and Sudan Black B dyes are respectively located at 508 and 602 nm, for clear comparison/confirmation, we therefore soaked a sample of **1** in EtOH solution of Congo Red and Sudan Black B at room temperature for 24 h. UV−vis absorption spectroscopy of the plasma suggests that the Congo Red dye was fully scavenged by **1**, while most of the Sudan Black B dye remained in the solution (see SI, Figure S43). When a sample of **2** was used instead of **1**, the scavenging effect is reverted. These results should be ascribed to the reversed affinity between the sorbate and sorbent before and after the postmodification. These experiments further proved that the imidazolium moieties in **1** are partially deprotonated for the formation of Pd[II]−NHCs in **2**. Moreover, these results indicate that the channels of the MONTs are accessible to large reagents typically used for catalysis, as the dye molecules have very large estimated cross sections. PXRD patterns suggest that the

framework structures remain intact, which can be used for catalytic application.

Because C−C bond formation reactions are very important in organic synthesis and the Pd complexes are a class of typical catalysts in these reactions, the Suzuki−Miyaura cross-coupling reaction of aryl halides with phenylboronic acids was carried out to evaluate the catalytic activity of **2**.[18] Heating a mixture of bromobenzene, phenylboronic acid, and K_2CO_3 in toluene at 70 °C for 5 h in the presence of solid **2** led to the formation of biphenyl in almost quantitative yield (Table 1, entry 1). Solid **2** can also catalyze the coupling reaction of a variety of phenylbromides with phenylboronic acids under the reaction conditions. As shown in Table 1, the electron-donating groups on phenylboronic acids can generate corresponding products in excellent yields, while the yield of the electron-withdrawing group on phenylboronic acid is moderate (Table 1, entries 2−4). When the substituents on phenylbromides are varied from electron-donating to electron-withdrawing groups, the corresponding product yields are almost quantitative (Table 1, entries 5−10). Catalyst **2** can also catalyze the coupling reaction of various phenyliodides and phenylboronic acids with excellent product yields (Table 1, entries 11−18). To make a comparison, Me_2L'/Pd, supported Pd catalyst, was used to conduct the catalytic experiment. However, the product yield was very low (Table 1, entry 19). To re-evaluate whether Pd atoms were grafted on the NHCs of **L′** or were simply adsorbed on the solid surface of **1**, $Pd(OAc)_2$ was used as a catalyst. However, the product yield was very low (Table 1, entry 20). To further eliminate the catalytic activity derived from the trace undetectable Pd[0] species, Pd/C was used as a catalyst. As expected, only a trace product was detected (Table 1, entry 21). These results unambiguously proved that the very high catalytic activity of **2** is from the NHCs anchored Pd[II] atoms as the catalytic efficiency of **2** is much better than the control catalysts. The catalytic efficiency of **2** is much superior to that of the less-

Table 1. Suzuki−Miyaura Coupling Reaction of Phenylhalides and Phenylboronic Acids[a]
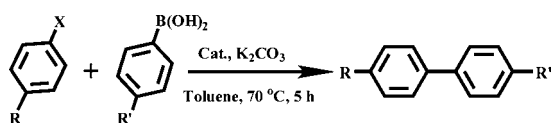
| entry	R	X	R′	yield (%)[b]
1	H	Br	H	>99
2	H	Br	CH_3	>99
3	H	Br	CH_3O	>99
4	H	Br	F	55 (0.3)
5	CH_3	Br	H	96 (1.3)
6	CH_3O	Br	H	97 (1.3)
7	CHO	Br	H	>99
8	CH_3CO	Br	H	>99
9	F	Br	H	>99
10	NO_2	Br	H	>99
11	H	I	H	>99
12	H	I	CH_3	>99
13	H	I	CH_3O	>99
14	H	I	F	75 (0.7)
15	CH_3	I	H	>99
16	CH_3O	I	H	>99
17	CH_3CO	I	H	>99
18	NO_2	I	H	>99
19	H	Br	H	42 (0.3)[c]
20	H	Br	H	22 (1)[d]
21	H	Br	H	1.1[e]
22	H	Br	H	98 (0.3)[f]

[a]Reaction conditions: Phenylhalide (1.0 mmol), phenylboronic acid (1.2 mmol), catalyst (0.005 mmol based on Pd), K_2CO_3 (2 mmol) in 5 mL of toluene were heated at 70 °C for 5 h. [b]Isolated yield, an average value of three runs (the value in the parentheses is error of the mean). [c]Catalyzed by Me_2L'/Pd. [d]Catalyzed by Pd(OAc)$_2$. [e]Catalyzed by Pd/C, based on GC analysis. [f]The sixth cycle.

porous catalyst with a similar building unit.[11] For example, the reaction of bromobenzene and 4-methoxyphenylboronic acid in the presence of solid **2** for 5 h quantitatively produces 4-methoxy-1,1′-biphenyl product (Table 1, entry 3), while the literature catalyst cannot prompt the reaction completely with 20-fold catalyst loading for 12 h.

After a mixture of **2**, K_2CO_3 and toluene was heated at 70 °C for 5 h under stirring, bromobenzene, phenylboronic acid, and additional K_2CO_3 were subsequently added into the hot filtrate. After heating the mixture at 70 °C for another 5 h, no product was detected. Moreover, ICP-MS did not detect a trace of palladium in the filtrate. These results demonstrate the heterogeneous catalytic behavior of **2**. Solid **2** can be easily recovered by centrifugation to remove the supernatant and washed with toluene and water for several times. The recovered catalyst was subsequently used in successive runs without deteriorating the catalytic efficiency (Table 1, entry 22). A PXRD pattern for the recovered solid suggests that the structural integrity of the catalyst was maintained during the catalytic process. TEM and XPS measurements of the recovered solid have confirmed that no Pd^0 nanoparticle was formed and the oxidation state of Pd remains divalent.

Because the palladium-catalyzed Heck coupling reaction is another powerful and versatile method to prepare arylated alkenes in fine chemical synthesis,[18b,c,19] the reaction between aryl halides and olefins was performed to further evaluate the

catalytic efficiency of **2**. As shown in Table 2, solid **2** is very active for the Heck coupling reaction of various phenylhalides

Table 2. Heck Coupling of Aryl Halides with Olefins[a]
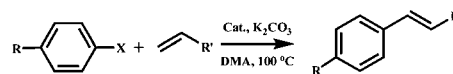
entry	X	R	R′	yield (%)[b]
1	Br	CHO	$COO(CH_2)_3CH_3$	>99
2	Br	CHO	Ph	>99
3	Br	NO_2	$COO(CH_2)_3CH_3$	>99
4	Br	NO_2	Ph	>99
5	I	H	$COO(CH_2)_3CH_3$	>99
6	I	H	Ph	>99
7	I	CH_3O	$COO(CH_2)_3CH_3$	>99
8	I	CH_3O	Ph	93(0.7)
9	I	NO_2	$COO(CH_2)_3CH_3$	>99
10	I	NO_2	Ph	>99
11	I	CH_3CO	$COO(CH_2)_3CH_3$	>99
12	I	CH_3CO	Ph	>99
13	I	H	$COO(CH_2)_3CH_3$	99(0.3)[c]

[a]Reaction conditions: aryl halide (1.0 mmol), olefin (1.2 mmol), catalyst (0.005 mmol based on Pd), and K_2CO_3 (2 mmol) in 5 mL of DMA were heated at 100 °C for 1 h. [b]Isolated yield, an average value of three runs (the value in the parentheses is error of the mean). [c]The sixth cycle.

and olefins in DMA in the presence of K_2CO_3 at 100 °C for 1 h with almost quantitative product yields. The recovered solid **2** also presents very high catalytic activity in successive runs (Table 2, entry 13).
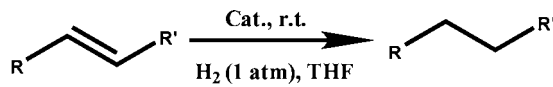
To further demonstrate the efficiency and versatility of catalyst **2**, the catalytic hydrogenation of various olefins was carried out as reduction of C−C multiple bonds is another important reaction in organic chemistry.[20] The reactions proceeded smoothly at room temperature with 0.5 mol % of **2** (based on Pd) under 1 atm H_2 atmosphere. As shown in Table 3, quantitative yields of the reduced products were achieved for a wide range of substrates after 1 h. The catalytic efficiency of recovered solid **2** does not decrease in the following six runs with quantitative yield (Table 3, entry 14). However, Me_2L'/Pd, Pd(OAc)$_2$, and Pd/C only generated trace product under the same conditions (Table 3, entries 15−17). We also used a large scale of (E)-ethyl cinnamate substrate with 0.005 mol % catalyst **2** to study the kinetic behavior and the stability. As shown in Figure 3, the turnover number (TON) reaches 13746 after 12 h without loss of the catalytic efficiency.

Finally, the catalytic potential of **2** was further demonstrated with reduction of nitrobenzene because of the important roles of aniline (Scheme 2).[21] It is interesting, with 0.5 mol % of **2** (based on Pd), nitrobenzene was fully reduced by H_2 under atmosphere pressure for 1 h at room temperature, leading to a quantitative yield of aniline. Moreover, the catalytic efficiency of the recovered solid **2** did not deteriorate in the successive six runs (>99% yield).

■ CONCLUSIONS

In summary, a two-component strategy was developed to design and construct a functional MONT. The formation of the MONT is directed by the coordination force between the bent organic ligands and tetra-coordinated zinc cations, while the

Table 3. Hydrogenation of Olefins[a]

Entry	Substrate	Product	Yield (%)[b]
1	(ethyl cinnamate)		>99
2	(H₃CO-phenyl cinnamate)		>99
3	(F-phenyl cinnamate)		98(0.3)
4	(cinnamaldehyde, CHO)		>99
5	(COCH₃)		>99
6	(CH₂OH)		99(0.7)
7	(CN)		>99
8	(styrene)		>99
9	(Br-styrene)		>99
10	(cyclopentene)		>99
11	(cyclohexene)		>99
12	(₃)		>99
13	(₅)		>99
14	(ethyl cinnamate)		>99[c]
15	(ethyl cinnamate)		<1[d]
16	(ethyl cinnamate)		5.3(0.2)[e]
17	(ethyl cinnamate)		<1[f]

[a]Reaction conditions: Olefin (0.1 mmol), H_2 (1 atm), and catalyst (0.0005 mmol based on Pd) in 3 mL of THF were stirred at room temperature for 1 h. [b]GC yield, an average value of three runs (the value in the parentheses is error of the mean). [c]The sixth cycle. [d]Catalyzed by Me_2L'/Pd. [e]Catalyzed by Pd(OAc)₂. [f]Catalyzed by Pd/C.

imidazolium moieties are used to control the functionality of MONT **1**, which can form NHCs and immobilize palladium atoms by unmasking the imidazolium moieties. The post-modified solid **2** synergizes the multiple functionalities of
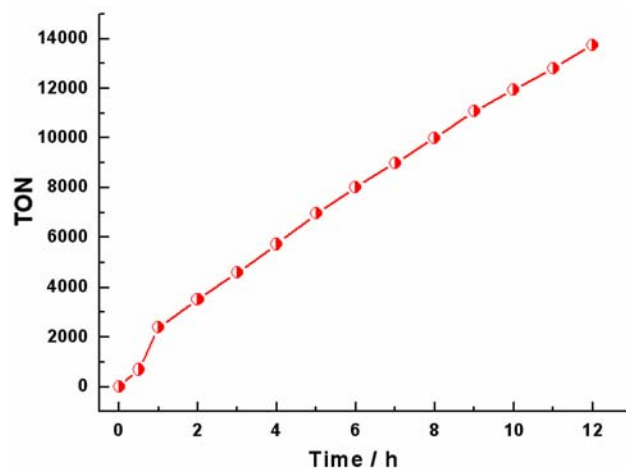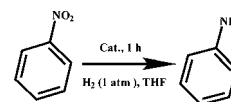

Figure 3. Hydrogenation of (E)-ethyl cinnamate catalyzed by **2** (the average values of three runs; the standard deviations are within 2%).

Scheme 2. Reduction of Nitrobenzene for the Formation of Aniline

MOFs, SNTs, and NHCs with high catalytic activity for a number of reactions, including Suzuki−Miyaura and Heck cross-coupling reactions, hydrogenation of olefins, and reduction of nitrobenzene. Reactions proceeded smoothly under mild conditions with very low catalyst loadings, while the constituent elements are much less efficient. The power to rationally immobilize metal sites for catalytic application highlights the approach as the very promising strategy to develop functional MONTs with unprecedented nature for potential applications.

■ EXPERIMENTAL SECTION

Materials and Methods. All of the chemicals were obtained from commercial sources and were used without further purification. Elemental analyses were performed on a ThermoFinnigan Flash EA 1112 elementary analyzer. GC−MS measurements were recorded on a SHIMADZU GCMS-QP2010. IR spectra were recorded from KBr pellets on an FTS-40 spectrophotometer. Inductively coupled plasma mass spectrometries (ICP-MS) were performed on an X-series-II instrument. Transmission electron microscopy (TEM) experiments were conducted using a JEOL JEM-1230 microscope operated at 80 kV. X-ray photoelectron spectroscopy (XPS) measurements were recorded on a VG ESCALAB MARK II system, and the C_{1s} line at 284.9 eV was used as the binding energy reference. Thermogravimetric analyses (TGA) were carried out on an SDT Q600 compositional analysis instrument from 30 to 800 °C under N_2 atmosphere at a heating rate of 10 °C/min. Powder X-ray diffraction data (PXRD) were recorded on a RIGAKU D/MAX 2550/PC for Cu Kα (λ = 1.5406 Å). Luminescent spectra for the solid samples were recorded with a Hitachi F4500 fluorescence spectrometer. Solid state UV−vis spectra were recorded with a 2802 UV/vis spectrophotometer. ^{1}H NMR and ^{13}C NMR spectra were recorded on a 500 MHz spectrometer in CDCl₃ or d^6-DMSO solution, and the chemical shifts were reported relative to internal standard TMS (0 ppm).

Synthesis of [ZnLCl₂]·8H₂O (1). The pH value of H_2LCl_2 (10 mg, 0.018 mmol) in 5 mL of water was adjusted to 7 using 1.0 mol/L NaOH aqueous solution, in which $Zn(NO_3)_2$·6H₂O (26 mg, 0.09 mmol) in 10 mL of EtOH was subsequently added. Colorless needle crystals of **1** that formed after three days at room temperature were

isolated by filtration, washed with EtOH and Et$_2$O, and dried in air (Yield: 53%). Anal. Calcd for C$_{23}$H$_{36}$N$_4$O$_{12}$Cl$_2$Zn (%): C, 39.64; H, 5.21; N, 8.04. Found: C, 40.33; H, 5.17; N, 7.88. IR (KBr pellet, ν/cm^{-1}): 1618(s), 1600(s), 1560(s), 1383(s), 1223(w), 1195(s), 1116(m), 1066(w), 912(w), 850(w), 785(m), 689(w), 615(w).

Synthesis of [ZnL$_{0.42}$L$'_{0.58}$Cl$_2$Pd$_{0.58}$(H$_2$O)$_{1.16}$]·9H$_2$O (2). A mixture of Pd(OAc)$_2$ (67.5 mg, 0.30 mmol), **1** (200 mg, 0.29 mmol), and THF (20 mL) was stirred at room temperature for 12 h and then refluxed for 24 h under an inert N$_2$ atmosphere. The resulting light-brown solid was filtered; washed with THF, MeOH, and Et$_2$O; and dried in air. Because **2** is insoluble in common organic solvents and water, a sample of **2** was decomposed by using an aqueous 5% HCl solution. The resulting solid was centrifuged, washed several times with H$_2$O, and dried in vacuum at 90 °C for 12 h. The residue was dissolved in d_6-DMSO for ^{1}H NMR spectroscopy. Anal. Calcd for C$_{23}$H$_{39.16}$N$_4$O$_{14.16}$Cl$_2$ZnPd$_{0.58}$ (%): C, 34.69; H, 4.96; N, 7.04. Found: C, 34.85; H, 4.81; N, 7.01. IR (KBr pellet, ν/cm^{-1}): 1618(s), 1599(s), 1560(s), 1383(s), 1223(w), 1194(s), 1115(m), 1066(w), 912(w), 850(w), 785(m), 688(w), 616(w).

Single-Crystal X-ray Data Collection and Structure Determination. The unit cell determination and data collection for the crystal of **1** were performed on an Oxford Xcalibur Gemini Ultra diffractometer with an Atlas detector. The data were collected using graphite-monochromatic enhanced ultra-Cu radiation (λ = 1.54178 Å) at 293 K. The data sets were corrected by empirical absorption correction using spherical harmonics, implemented in the SCALE3 ABSPACK scaling algorithm.[22] The structure was solved by direct methods and refined by full-matrix least-squares methods with the SHELX-97 program package.[23] All nonsolvent atoms were located successfully from Fourier maps. The solvent molecules in compound **1** are highly disordered, and the SQUEEZE subroutine of the PLATON software suite was used to remove the scattering from the highly disordered guest molecules.[24] The resulting new files were used to further refine the structure.

Crystal data for 1: C$_{23}$H$_{19}$Cl$_2$N$_4$O$_4$Zn, M = 551.69, hexagonal, space group $P6_2$22, a = 30.0265(11) Å, c = 7.7081(4) Å, V = 6018.5(4) Å^3, Z = 6, ρ = 0.913 g.cm^{-3}, μ = 2.269 mm^{-1}, R1 = 0.0754, wR2 = 0.1801, S = 1.075 and Flack parameter = 0.03(7).

A Typical Procedure for the Dye Adsorption Experiment. Compound **1** (10 mg) was added into a 10 mL of EtOH solution of Congo Red (100 mg·L^{-1}) under stirring at room temperature for 24 h. The solution was centrifuged, and the plasma was analyzed by UV−vis absorption spectroscopy after the solution was diluted to 1/10 of the original. The amount of adsorbed dyes was calculated from the following mass balance equation:

$$Q_{ad} = \frac{(C_0 - C_{ad})}{m}V$$

where Q_{ad} (mmol/g) is the amount of adsorbed dyes by adsorbent **1**, C_0 is the initial concentration of dyes in EtOH (mmol/L), C_{ad} is the concentration of dyes after adsorption (mmol/L), V is the volume of the solution (L), and m is the mass of adsorbent **1** (g).

The Procedure for Selective Adsorption of Congo Red and Sudan Black B. Compound **1** (10 mg) was added into a 10 mL of EtOH solution containing Congo Red (1.0 mg) and Sudan Black B (0.4 mg) under stirring at room temperature for 24 h. The solution was centrifuged, and the plasma was analyzed by UV−vis absorption spectroscopy after the solution was diluted to 1/10 of the original.

A Typical Procedure for the Suzuki−Miyaura Coupling Reaction Catalyzed by Solid 2. Bromobenzene (1.0 mmol), phenylboronic acid (1.2 mmol), K$_2$CO$_3$ (2 mmol), and **2** (0.005 mmol based on Pd) in 5 mL of toluene were stirred at 70 °C for 5 h under air atmosphere. After the reaction was complete, the reaction mixture was cooled down to room temperature, centrifuged, and extracted with ethyl acetate/water. The organic layer was separated, dried over anhydrous MgSO$_4$, and concentrated in a vacuum. The residue was subjected to chromatography on silica gel using hexane as eluent to give the isolated yield.

A Typical Procedure for the Heck Coupling Reaction Catalyzed by Solid 2. Aryl halide (1.0 mmol), n-butyl acrylate

(1.2 mmol), K$_2$CO$_3$ (2 mmol), and **2** (0.005 mmol based on Pd) in 5 mL of DMA were stirred at 100 °C for 1 h under air atmosphere. After the reaction was complete, the reaction mixture was cooled down to room temperature, centrifuged, and extracted with ethyl acetate/water. The organic layer was separated, dried over anhydrous MgSO$_4$, and concentrated in vacuum. The residue was subjected to chromatography on silica gel using hexane as eluent to give the isolated yield.

A Typical Procedure for the Reduction of Olefins Catalyzed by Solid 2. A mixture of catalyst **2** (0.0005 mmol based on Pd) and olefin (0.1 mmol) in THF (3 mL) under 1 atm hydrogen atmosphere was stirred at room temperature for 1 h. The identity of the product was determined by GC−MS and compared with the authentic samples analyzed under the same conditions; the yield was obtained by GC analysis with a flame-ionization detector (FID) using a capillary SE-54 column.

Study of the TONs for Hydrogenation of (E)-Ethyl Cinnamate Catalyzed by Solid 2. A mixture of catalyst **2** (0.005 mmol based on Pd) and (E)-ethyl cinnamate (100 mmol) in THF (50 mL) under 1 atm hydrogen atmosphere was stirred at room temperature for 12 h. Aliquots were regularly withdrawn for GC analysis to determine the yield of ethyl 3-phenylpropanoate and TONs (TON is defined as the mole ratio of the yielded product to the catalyst).

The Procedure for the Reduction of Nitrobenzene Catalyzed by Solid 2. A mixture of catalyst **2** (0.0005 mmol based on Pd) and nitrobenzene (0.1 mmol) in THF (3 mL) under 1 atm hydrogen atmosphere was stirred at room temperature for 1 h. The identity of the product was determined by GC−MS and compared with the authentic samples analyzed under the same conditions, and the yield was obtained by GC analysis with a flame-ionization detector (FID) using a capillary SE-54 column.

■ ASSOCIATED CONTENT

Ⓢ Supporting Information

Experimental procedures, additional figures, data and tables, and crystallographic data. This material is available free of charge via the Internet at http://pubs.acs.org.

■ AUTHOR INFORMATION

Corresponding Author

cdwu@zju.edu.cn

Notes

The authors declare no competing financial interest.

■ ACKNOWLEDGMENTS

■ REFERENCES

(1) Iijima, S. Nature 1991, 354, 56.

(2) (a) Goldberger, J.; Fan, R.; Yang, P. Acc. Chem. Res. 2006, 39, 239. (b) Sgobba, V.; Guldi, D. M. Chem. Soc. Rev. 2009, 38, 165.

(3) (a) Blau, W. J.; Fleming, A. J. Science 2004, 304, 1457. (b) Dalgarno, S. J.; Cave, G. W. V.; Atwood, J. L. Angew. Chem., Int. Ed. 2006, 45, 570. (c) Pantos, G. D.; Pengo, P.; Sanders, J. K. M. Angew. Chem., Int. Ed. 2007, 46, 194. (d) Hao, S.; Zhou, G.; Duan, W.; Wu, J.; Gu, B.-L. J. Am. Chem. Soc. 2008, 130, 5257. (e) Tang, Y.; Zhou, L.; Li, J.; Luo, Q.; Huang, X.; Wu, P.; Wang, Y.; Xu, J.; Shen, J.; Liu, J. Angew. Chem., Int. Ed. 2010, 49, 3920. (f) Xiong, W.; Du, F.; Liu, Y.; Perez, A., Jr.; Supp, M.; Ramakrishnan, T. S.; Dai, L.; Jiang, L. J. Am. Chem. Soc. 2010, 132, 15839.

(4) (a) Kitagawa, S.; Kitaura, R.; Noro, S.-i. Angew. Chem., Int. Ed. 2004, 43, 2334. (b) Férey, G.; Serre, C. Chem. Soc. Rev. 2009, 38, 1380. (c) Murray, L. J.; Dincă, M.; Long, J. R. Chem. Soc. Rev. 2009,

38, 1294. (d) Li, J.-R.; Kuppler, R. J.; Zhou, H.-C. *Chem. Soc. Rev.* **2009**, *38*, 1477. (e) Chen, B.; Xiang, S. C.; Qian, G. *Acc. Chem. Res.* **2010**, *43*, 1115. (f) Kreno, L. E.; Leong, K.; Farha, O. K.; Allendorf, M.; Van Duyne, R. P.; Hupp, J. T. *Chem. Rev.* **2012**, *112*, 1105. (g) Cui, Y.; Yue, Y.; Qian, G.; Chen, B. *Chem. Rev.* **2012**, *112*, 1126. (h) Ma, L.; Abney, C.; Lin, W. *Chem. Soc. Rev.* **2009**, *38*, 1248. (i) Lee, J.; Farha, O. K.; Roberts, J.; Scheidt, K. A.; Nguyen, S. T.; Hupp, J. T. *Chem. Soc. Rev.* **2009**, *38*, 1450. (j) Corma, A.; Garcia, H.; Llabrés, i; Xamena, F. X. *Chem. Rev.* **2010**, *110*, 4606. (k) Yoon, M.; Srirambalaji, R.; Kim, K. *Chem. Rev.* **2012**, *112*, 1196. (l) Wu, H.; Gong, Q.; Olson, D. H.; Li, J. *Chem. Rev.* **2012**, *112*, 836. (m) Jiang, H.-L.; Xu, Q. *Chem. Commun.* **2011**, *47*, 3351.

(5) (a) Fang, Q.-R.; Zhu, G.-S.; Jin, Z.; Ji, Y.-Y.; Ye, J.-W.; Xue, M.; Yang, H.; Wang, Y.; Qiu, S.-L. *Angew. Chem., Int. Ed.* **2007**, *46*, 6638. (b) Xiang, S.; Huang, J.; Li, L.; Zhang, J.; Jiang, L.; Kuang, X.; Su, C.-Y. *Inorg. Chem.* **2011**, *50*, 1743. (c) Lin, Q.; Wu, T.; Zheng, S.-T.; Bu, X.; Feng, P. *Chem. Commun.* **2011**, *47*, 11852.

(6) Thanasekaran, P.; Luo, T.-T.; Lee, C.-H.; Lu, K.-L. *J. Mater. Chem.* **2011**, *21*, 13140.

(7) (a) Cui, Y.; Lee, S. J.; Lin, W. *J. Am. Chem. Soc.* **2003**, *125*, 6014. (b) Pickering, A. L.; Seeber, G.; Long, D.-L.; Cronin, L. *Chem. Commun.* **2004**, 136. (c) Fei, Z.; Zhao, D.; Geldbach, T. J.; Scopelliti, R.; Dyson, P. J.; Antonijevic, S.; Bodenhausen, G. *Angew. Chem., Int. Ed.* **2005**, *44*, 5720. (d) Dai, F.; He, H.; Sun, D. *J. Am. Chem. Soc.* **2008**, *130*, 14064. (e) Huang, X.-C.; Luo, W.; Shen, Y.-F.; Lin, X.-J.; Li, D. *Chem. Commun.* **2008**, 3995. (f) Luo, T.-T.; Wu, H.-C.; Jao, Y.-C.; Huang, S.-M.; Tseng, T.-W.; Wen, Y.-S.; Lee, G.-H.; Peng, S.-M.; Lu, K.-L. *Angew. Chem., Int. Ed.* **2009**, *48*, 9461. (g) Otsubo, K.; Wakabayashi, Y.; Ohara, J.; Yamamoto, S.; Matsuzaki, H.; Okamoto, H.; Nitta, K.; Uruga, T.; Kitagawa, H. *Nat. Mater.* **2011**, *10*, 291.

(8) (a) Nair, V.; Menon, R. S.; Biju, A. T.; Sinu, C. R.; Paul, R. R.; Jose, A.; Sreekumar, V. *Chem. Soc. Rev.* **2011**, *40*, 5336. (b) Fortman, G. C.; Nolan, S. P. *Chem. Soc. Rev.* **2011**, *40*, 5151. (c) Nair, V.; Vellalath, S.; Bahu, B. P. *Chem. Soc. Rev.* **2008**, *37*, 2691.

(9) (a) O'Brien, J. M.; Lee, K.-s.; Hoveyda, A. H. *J. Am. Chem. Soc.* **2010**, *132*, 10630. (b) Teyssot, M.-L.; Chevry, A.; Traïkia, M.; El-Ghozzi, M.; Avignant, D.; Gautier, A. *Chem.—Eur. J.* **2009**, *15*, 6322. (c) Díez-González, S.; Nolan, S. P. *Angew. Chem., Int. Ed.* **2008**, *47*, 8881. (d) Ranganath, K. V. S.; Kloesges, J.; Schäfer, A. H.; Glorius, F. *Angew. Chem., Int. Ed.* **2010**, *49*, 7786. (e) Gottumukkala, A. L.; de Vries, J. G.; Minnaard, A. J. *Chem.—Eur. J.* **2011**, *17*, 3091.

(10) (a) Oisaki, K.; Li, Q.; Furukawa, H.; Czaja, A. U.; Yaghi, O. M. *J. Am. Chem. Soc.* **2010**, *132*, 9262. (b) Crees, R. S.; Cole, M. L.; Hanton, L. R.; Sumby, C. J. *Inorg. Chem.* **2010**, *49*, 1712. (c) Lee, J. Y.; Roberts, J. M.; Farha, O. K.; Sarjeant, A. A.; Scheidt, K. A.; Hupp, J. T. *Inorg. Chem.* **2009**, *48*, 9971. (d) Han, L.; Zhang, S.; Wang, Y.; Yan, X.; Lu, X. *Inorg. Chem.* **2009**, *48*, 786. (e) Chun, J.; Jung, G.; Kim, H. J.; Park, M.; Lah, M. S.; Son, S. U. *Inorg. Chem.* **2009**, *48*, 6353. (f) Kong, G.-Q.; Wu, C.-D. *CrystEngComm* **2012**, *14*, 847.

(11) Kong, G.-Q.; Xu, X.; Zou, C.; Wu, C.-D. *Chem. Commun.* **2011**, *47*, 11005.

(12) Spek, A. L. *PLATON, A Multipurpose Crystallographic Tool*; Utrecht University: Utrecht, The Netherlands, 2008.

(13) Mukhopadhyay, K.; Sarkar, B. R.; Chaudhari, R. V. *J. Am. Chem. Soc.* **2002**, *124*, 9692.

(14) Liu, G.; Hou, M.; Wu, T.; Jiang, T.; Fan, H.; Yang, G.; Han, B. *Phys. Chem. Chem. Phys.* **2011**, *13*, 2062.

(15) Yang, H.; Han, X.; Li, G.; Wang, Y. *Green Chem.* **2009**, *11*, 1184.

(16) (a) Jiang, H.-L.; Tatsu, Y.; Lu, Z.-H; Xu, Q. *J. Am. Chem. Soc.* **2010**, *132*, 5586. (b) Han, S.; Wei, Y.; Valente, C.; Lagzi, I.; Gassensmith, J. J.; Coskun, A.; Stoddart, J. F.; Grzybowski, B. A. *J. Am. Chem. Soc.* **2010**, *132*, 16358. (c) Lan, Y.-Q.; Jiang, H.-L.; Li, S.-L.; Xu, Q. *Adv. Mater.* **2011**, *23*, 5015.

(17) Ahmad, R.; Wong-Foy, A. G.; Matzger, A. J. *Langmuir* **2009**, *25*, 11977.

(18) (a) Fihri, A.; Bouhrara, M.; Nekoueishahraki, B.; Basset, J.-M.; Polshettiwar, V. *Chem. Soc. Rev.* **2011**, *40*, 5181. (b) Balanta, A.; Godard, C.; Claver, C. *Chem. Soc. Rev.* **2011**, *40*, 4973. (c) Noël, T.; Buchwald, S. L. *Chem. Soc. Rev.* **2011**, *40*, 5010.

(19) (a) Cartney, D. M.; Guiry, P. J. *Chem. Soc. Rev.* **2011**, *40*, 5122. (b) Fu, Z.; Huang, S.; Su, W.; Hong, M. *Org. Lett.* **2010**, *12*, 4992.

(20) (a) Jurčík, V.; Nolan, S. P.; Cazin, C. S. J. *Chem.—Eur. J.* **2009**, *15*, 2509. (b) Erathodiyil, N.; Ooi, S.; Seayad, A. M.; Han, Y.; Lee, S. S.; Ying, J. Y. *Chem.—Eur. J.* **2008**, *14*, 3118. (c) Ornelas, C.; Aranzaes, J. R.; Salmon, L.; Astruc, D. *Chem.—Eur. J.* **2008**, *14*, 50.

(21) Li, J.; Shi, X.-Y.; Bi, Y.-Y.; Wei, J.-F.; Chen, Z.-G. *ACS Catal.* **2011**, *1*, 657.

(22) *CrysAlisPro*, version 171.34.44; Oxford Diffraction Ltd.: Oxfordshire, U.K., 2010.

(23) Sheldrick, G. M. *Program for Structure Refinement*: University of Göttingen, Germany, 1997.

(24) Spek, A. L. *J. Appl. Crystallogr.* **2003**, *36*, 7.